Stabilization of High-Valent Terminal-Oxo Complexes: Interplay of d-Orbital Occupancy and Coordination Geometry

Nathanael L. P. Fackler,† Songsheng Zhang,† and Thomas V. O'Halloran*,†,‡

Departments of Chemistry and Biochemistry, Molecular Biology and Cell Biology Northwestern University, Evanston, Illinois 60208-3113

Received September 5, 1995

To design highly selective catalysts for oxidation of organic compounds, we are probing the electronic,[1] thermodynamic,[2,3] and geometric properties of the reactive species. Chelating ligands that increase the stability of metal−oxo intermediates can allow fine-tuning of chemo- and regioselectivity in the oxo- and electron-transfer steps.[4] Previous structural and mechanistic studies of chelators containing amide donors[5−7] underscore how ligand basicity can stabilize high oxidation state metal centers; however, here we focus on the importance of coordination geometry. We report the unusual geometry of a novel Ru^{V} oxidation catalyst that is formally analogous to a perferryl species, a frequently postulated iron−oxo intermediate in biological oxidations.[8] By comparison with the related Ru^{VI}−oxo complex, we show that the preferred coordination geometry of these oxo-terminal complexes depends strongly on the formal d-electron occupancy of the metal−oxo π*-orbitals. These results have important implications for the design of ligands that stabilize specific intermediates in catalytic reactions. Ligands such as porphyrins and macrocyclic amides, which impose a rigid planar array of four donor atoms, clearly stabilize d^0−d^2 metal−oxo centers but may destabilize electron-rich systems, such as the hypothetical d^3 perferryl species, relative to more flexible ligands that contain similar donor atoms. These results also suggest a means by which subtle conformational restraints imposed by oxo-transfer enzymes on the geometry of metal cofactors can significantly tune the reactivity of the metal−oxo intermediate.

Direct reaction of RuO_4^- with H_4PHAB[7] gives the paramagnetic monooxoruthenium complex Pr_4N[Ru(O)PHAB] (**1**).[9] Subsequent oxidation by Ce^{IV} yields the diamagnetic monooxo complex [Ru(O)PHAB] (**2**).[10] As expected, the $\nu_{M=O}$ stretch

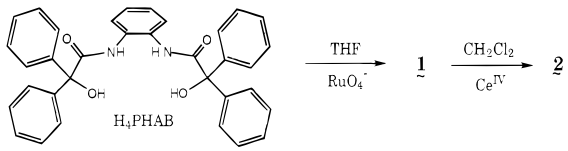

shifts to higher frequency upon oxidation (887 vs 935 cm^{-1} for **1** and **2**, respectively).[11] Differences in the IR spectra, however, indicate that significant structural changes occur upon oxidation: KBr pellets of **1** exhibit two amide $\nu_{C=O}$ stretches at 1670 and 1630 cm^{-1}, but only a single amide $\nu_{C=O}$ stretch at 1704 cm^{-1} is evident for **2**. X-ray diffraction analysis reveals that **2** is a square-pyramidal (SP) Ru^{VI}−monooxo species,[10] but **1** is a distorted trigonal-bipyramidal (TBP) Ru^{V}−oxo complex[9] (Figure 1). Although a variety of *dioxo*−Ru^{VI} species are known,[12] **2** represents the first structurally characterized example of Ru^{VI} with a single terminal oxo group. The central Ru atom sits 0.70 Å above the N_2O_2 basal plane, and the terminal oxo occupies the apical position. The Ru^{VI}═O bond in **2** is shorter than that in **1** and approaches that observed in a couple of dioxo−Ru^{VI} complexes.[13,14]

Comparisons of the alkoxo− and amido−metal bond lengths clearly indicate lower symmetry in **1** than in **2**. The two Ru−N bond lengths in **1** differ by 0.07 Å, and the two Ru−O bond lengths differ by 0.1 Å, whereas the analogous parameters in **2** are indistinguishable from one another at the 3σ limit. The four donor atoms of the PHAB ligand are significantly distorted from planarity in **1** relative to **2**, exhibiting mean deviations of the N_2O_2 planes of 0.1830 and 0.03 Å, respectively. The trigonal plane in **1**, defined by Ru−N1−O1−O3 (see dotted line in Figure 1) has a mean deviation of 0.05 Å, with Ru sitting 0.003 Å out of the plane and the axial N2−Ru−O2 subtending an angle of 155.2(1)°. The terminal oxo occupies an equatorial position, analogous to that reported for the only other structurally characterized monooxo−Ru^{V} complex, $Pr_4N[Ru^{V}(O)(O_2CCEt_2)_2]$.[15]

While the barrier for interconversion of metal complexes between SP and TBP geometries can be quite small,[16] this is not the case when metal−ligand multiple bonds are present. Several differences in **1** and **2** indicate that the thermodynamic preference for a particular five-coordinate geometry depends on the occupancy of orbitals with significant d-character. First, the distortion of the ligand in **1** is retained in solution and

* Corresponding author: Department of Chemistry, Northwestern University, 2145 Sheridan Rd., Evanston, IL 60208-3113. Phone: (708) 491-5060. Fax: (708) 491-7713.

† Department of Chemistry.

‡ Department of Biochemistry, Molecular Biology and Cell Biology.

(1) Nugent, W. A.; Mayer, J. M. *Metal−Ligand Multiple Bonds*; Wiley-Interscience: New York, 1988.

(2) Holm, R. H. *Chem. Rev.* **1987**, *87*, 1401−1449.

(3) Cook, G. K.; Mayer, J. M. *J. Am. Chem. Soc.* **1995**, *117*, 7139−7156.

(4) Jacobsen, E. N.; Zhang, W.; Güler, M. L. *J. Am. Chem. Soc.* **1991**, *113*, 6703−6704.

(5) Margerum, D. W. *Pure Appl. Chem.* **1983**, *55*, 23−34.

(6) Collins, T. J. *Acc. Chem. Res.* **1994**, *27*, 279−285.

(7) MacDonnell, F. M.; Fackler, N. L. P.; O'Halloran, T. V. *J. Am. Chem. Soc.* **1994**, *116*, 7431−7432.

(8) (a) Gunter, M. J.; Turner, P. *Coord. Chem. Rev.* **1991**, *108*, 115−161. (b) Liu, K. E.; Wang, D.; Huynh, B. H.; Edmondson, D. E.; Salifoglou, A.; Lippard, S. J. *J. Am. Chem. Soc.* **1994**, *116*, 7465−7466. (c) Lee, S. K.; Fox, B. G.; Froland, W. A.; Lipscomb, J. D.; Münck, E. *J. Am. Chem. Soc.* **1993**, *115*, 6450−6451. (d) Posner, G. H.; Cumming, J. N.; Ploypradith, P.; Oh, C. H. *J. Am. Chem. Soc.* **1995**, *117*, 5885−5886.

(9) (a) Anal. Calcd for $Pr_4N[Ru^{V}(O)PHAB]$, $C_{46}H_{52}N_3O_5Ru$: C, 66.73; H, 6.33; N, 5.07. Found: C, 66.18; H, 6.26; N, 5.02 (Oneida). IR of a KBr pellet: ($\nu_{C=O}$) 1670, 1630 cm^{-1}; ($\nu_{M=O}$) 887 cm^{-1}. UV−vis (CH_2Cl_2): λ_{max} (nm) (ϵ, M^{-1} cm^{-1}) 336 (3335), 420 (968), 538 (270). The synthetic procedure is available as supporting information. (b) Black crystals of **1** were grown by slow evaporation of an acetonitrile solution at room temperature. **1** crystallizes in the space group $P2_1/n$, with a = 11.981(2) Å, b = 11.245(2) Å, c = 30.082(8) Å, β = 98.90(2)°, V = 4004(3), ρ_{ca}3l$_c$ = 1.373 g cm^{-3}, and Z = 4. Data collection at −120 °C from 2.8 ≤ 2θ ≤ 48° provided 4033 reflections with $I > 3.00\sigma(I)$. The structure was solved by Patterson methods (SHELXS) and refined in TEXSAN 5.0 with 654 variables to a final R (R_w) value 0.035 (0.036).

(10) (a) Anal. Calcd for $[Ru^{VI}(O)PHAB]$, $C_{34}H_{24}N_2O_5Ru$: C, 63.65; H, 3.77; N, 4.36. Found: C, 63.34; H, 3.77; N, 4.32 (Oneida). IR of a KBr pellet: ($\nu_{C=O}$) 1704 cm^{-1}; ($\nu_{M=O}$) 931 cm^{-1}. UV−vis (CH_2Cl_2): λ_{max} (nm) (ϵ, M^{-1} cm^{-1}) 398 (3388), 458 (3436), 616 (1168). (b) Dark green crystals of **2**·$(CH_3)_2CO$, grown from a concentrated acetone solution at −4 °C, were mounted on a glass fiber under oil (paratone N) to prevent solvent loss. **2** crystallizes in the space group $P\bar{1}$, with a = 9.259(1) Å, b = 12.385-(1) Å, c = 14.143(3) Å, α = 102.25(1)°, β = 91.69(1)°, γ = 103.58(1), V = 1535.2(8), ρ_{calc} = 1.513 g cm^{-3}, and Z = 2. Data collection at −120 °C from 2.8 ≤ 2θ ≤ 55° provided 5874 reflections with $I > 3.00\sigma(I)$. The structure was solved by Patterson methods (SHELXS) and refined in TEXSAN 5.0 with 536 variables to a final R (R_w) value 0.024 (0.031).

(11) Isotopic labeling was achieved by reducing an acetonitrile solution of **1** (100 mg, 0.12 mmol) with a substoichiometric aliquot of Ph_3P under a nitrogen atmosphere. After stirring overnight, $^{18}O_2$-labeled dioxygen (99%) was introduced. Precipitation with diethyl ether and crystallization of the powder from acetonitrile provided partially labeled (∼34%) **1**. IR (KBr pellet): ($\nu_{M=O}$) 885 cm^{-1}; ($\nu_{M=O*}$) 841 cm^{-1} (calcd $\nu_{M=O*}$, 841 cm^{-1}). Ce^{IV} oxidation of ^{18}O-labeled **1** in CH_2Cl_2, followed by crystallization of the dark green oil from acetone, provided pure, partially labeled (∼13%) **2**. IR (KBr pellet): ($\nu_{M=O}$) 926 (941 sh) cm^{-1}; ($\nu_{M=O*}$) 887 cm^{-1} (calcd $\nu_{M=O*}$, 876 (895 sh) cm^{-1}).

(12) Che, C.-M.; Yam, V. W.-W. In *Advances in Inorganic Chemistry*; Sykes, A. G., Ed.; Academic Press, Inc.: San Diego, 1992; Vol. 39, pp 233−325.

(13) Perrier, S.; Kochi, J. K. *Inorg. Chem.* **1988**, *27*, 4165−4173.

(14) Dovletoglou, A.; Adeyemi, S. A.; Lynn, M. H.; Hodgson, D. J.; Meyer, T. J. *J. Am. Chem. Soc.* **1990**, *112*, 8989−8990.

(15) Dengel, A. C.; Griffith, W. P.; O'Mahoney, C. A.; Williams, D. J. *J. Chem. Soc., Chem. Commun.* **1989**, 1720−1721.

(16) Holmes, R. R. *Prog. Inorg. Chem.* **1984**, *32*, 119.

0002-7863/96/1518-0481$12.00/0

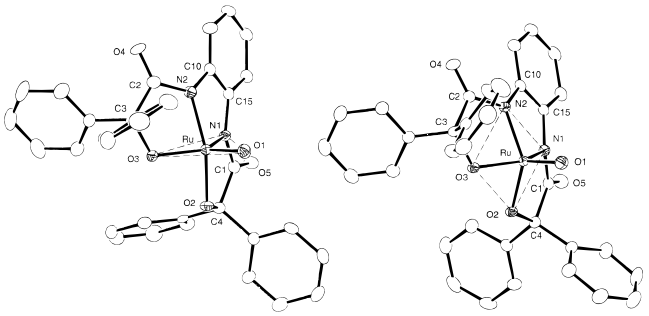

Figure 1. ORTEP representations of the anion **1** and the neutral complex **2**, showing 50% probability ellipsoids. Solvate molecules and hydrogen atoms are omitted for clarity. Selected bond distances (Å) and angles (deg) are as follows. (Left) **1**: Ru−O1, 1.702(3); Ru−O2, 2.007(3); Ru−O3, 1.897(3); Ru−N1, 1.907(4); Ru−N2, 1.978(4); O2−Ru−N2, 155.2(1), O3−Ru−O1, 117.3(1); O3−Ru−N1, 130.4(1); O1−Ru−N1, 111.8(2). (Right) **2**: Ru−O1, 1.661(1); Ru−O(2), 1.899(1); Ru−O3, 1.895(1); Ru−N1, 1.929(2); Ru−N2, 1.923(2); O2−Ru−O3, 84.23(6); O2−Ru−N1, 82.17(6); O3−Ru−N2, 82.83(6); N1−Ru−N2, 80.52(7); O1−Ru−O3, 110.82(6); O1−Ru−O2, 113.19(7); O1−Ru−N1, 109.99(7); O1−Ru−N2, 111.09(7); O2−Ru−N2, 135.63(6); O3−Ru−N1, 139.12(6).

therefore is not a result of crystal packing forces. FT-IR of **1** in CH_2Cl_2 reveals both of the intense amide $\nu_{C=O}$ stretches observed in the crystalline material, albeit shifted to higher energy.[17] Second, the PHAB ligand framework undergoes an atypical distortion to maintain the TBP geometry of **1**. All other PHAB complexes characterized to date form SP complexes, including **2**, Ph_4P[Mn(O)PHAB] (**3**), and the dimer Li_2[MnPHAB]$_2$ (**4**).[7]

The altered ligand conformation of **1** is also apparent in pyramidalization or χ_N values:[18] moderate distortion of one amide (N2) is observed. The N1 amide and all of the amides in the other SP PHAB complexes **2**−**4** maintain the planarity characteristic of normal sp^2 hybridization.[18] The distortion in N2 leads to an unfavorable reduction in resonance stabilization from both the carbonyl and ligand phenyl backbone,[19] evident as a higher frequency $\nu_{C=O}$ stretch for amide N2 than for the planar amide N1. A compensating Ru−N2 bonding interaction cannot account for the energetic cost of this ligand distortion. While the distortion does make N2 a stronger donor ligand,[20] it sits 0.07 Å further from the Ru center than amide N1, suggestive of a weaker M−L bond. Thus, in spite of an unfavorable ligand strain energy, the distorted geometry in **1** is closer to TBP than SP.

Extended Hückel calculations[21] suggest that in the absence of ligand strain, a d^3 metal−oxo center will generally prefer TBP over SP geometry (Chart 1). This stabilization is reflected in a lower energy for the occupied component of the d_{xz},d_{yz} pair. In both the SP and TBP geometries, the HOMO of a d^3

Chart 1

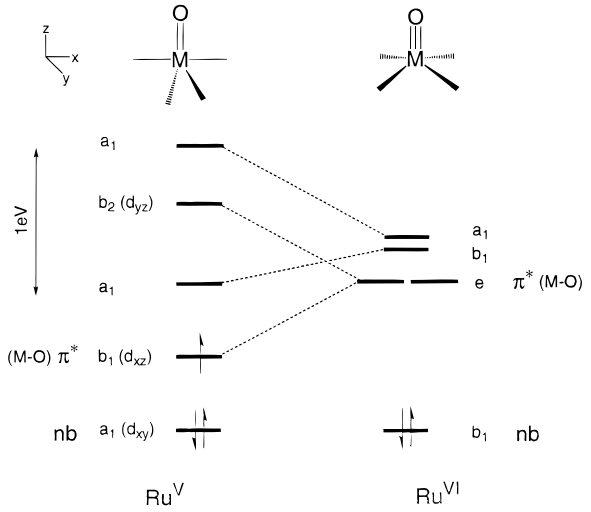

M═O center is orthogonal to the equatorial ligand plane and antibonding with respect to the oxo. In the SP geometry, M−L σ* contributions further destabilize the e set (d_{xz},d_{yz}), which are hybridized away from the basal ligands toward the apical oxygen.[22] By increasing one of the L−M−L angles to 180°, as in the TBP geometry, the equatorial M−L σ* interactions are effectively removed from the HOMO. This model is consistent with the physical data: **2** is diamagnetic, providing a sharp ^{1}H-NMR,[23] while **1** is paramagnetic [μ_{eff} (298 K) = 2.0 μ_B] and gives rise to an isotropic solid state EPR spectrum [g (77 K) = 1.98]. The dependence of the geometry of **1** on the d-orbital occupation of M−O π*-orbitals leads us to suggest that other d^3 or d^4 L_4M═X complexes, where X is oxo, nitrido, or sulfido and L_4 is a macrocycle or porphyrin radical, may be significantly more stable in TBP relative to SP or octahedral geometries.

The stability of **1** and **2** is reflected in the M−O bond energy, which can be estimated from reactivity comparisons.[24] Both complexes facilitate C−H bond activation and oxygen atom transfer reactions, oxidizing benzyl alcohol to the aldehyde and Ph_3P to Ph_3P═O. Notably, neither complex oxidizes styrene to the oxide. The metal−oxo bond energies of **1** and **2** are clearly less than the Ph_3P−O bond energy of 135 kcal/mol.[25] Furthermore, the air oxidation of Ph_3P is catalyzed by **1**, emphasizing its unusual stability.[26] Evaluations of the roles of electronic structure and coordination geometry in these oxidation mechanisms are underway.

Acknowledgment. We thank C. Stern, J. Ibers, J. Bollinger, M. Mansuetto, O. Eisenstein, and F. MacDonnell for helpful discussions. This work was supported by NSF (Presidential Young Investigator Award CHE8657704), the Alfred P. Sloan Foundation, and a Camille and Henry Dreyfus Teacher Scholar Award to T.V.O.

Supporting Information Available: Synthetic procedures, atomic positional parameters, intramolecular bond distances and angles, complete ORTEP drawings, and infrared spectra for **1** and **2** (21 pages); observed and calculated structure factors (68 pages). This material is contained in many libraries on microfiche, immediately follows this article in the microfilm version of the journal, can be ordered from the ACS, and can be downloaded from the Internet; see any current masthead page for ordering information and Internet access instructions.

JA953051I

(17) Solution FT-IR spectra were obtained using a 0.050 mm KBr solution cell with CH_2Cl_2 as solvent. Difference spectra (in CH_2Cl_2): ($\nu_{C=O}$) **1**, 1713 and 1642 cm^{-1}; **2**, 1710 cm^{-1}.

(18) The pyramidalization term χ_N is defined as follows (Winkler, F. K.; Dunitz, J. D. *J. Mol. Biol.* **1971**, *59*, 169−182): $\chi_N = (\omega_2 - \omega_3 + \pi)$ mod 2π, where ω_2 = O−C−N−M and ω_3 = O−C−N−C. χ_N maximizes at 60° and can be understood as the point at which the central nitrogen atom adopts a tetrahedral geometry. The following torsion angles and Dunitz parameters are for amides numbered as N1−C1−O5 and N2−C2−O4, respectively: **1**, ω_2 = −170.8°, −173.6°, ω_3 = 8.5°, −22.7°, χ_{N1} = 0.7°, and χ_{N2} = 29.1°; **2**, ω_2 = 179.3°, −178.1°, ω_3 = 18.1°, −18.1°, χ_{N1} = −18.8°, and χ_{N2} = 20.2°. The χ_N values observed for complexes **3** and **4** respectively are χ_{N1} = 5.4°, χ_{N2} = −7.9° and χ_{N1} = 10.8°, χ_{N2} = −17.8°, χ_{N3} = −15.5°, χ_{N4} = 16.8°.

(19) Itai, A.; Toriumi, Y.; Saito, S.; Kagechika, H.; Shudo, K. *J. Am. Chem. Soc.* **1992**, *114*, 10649−10650.

(20) Anson, F. C.; Collins, T. J.; Gipson, S. L.; Keech, J. T.; Kraft, T. E.; Peake, G. T. *J. Am. Chem. Soc.* **1986**, *108*, 6593−6605.

(21) EH calculations were performed on idealized RuH_4O models of **1** (C_{2v}) and **2** (C_{4v}) in CACAO v. 3.0. See: Mealli, C.; Proserpio, D. M. *J. Chem. Educ.* **1990**, *67*, 399−402 and references therein. The *trans* basal angles of the square pyramid were defined as 135°, the average of that found in the X-ray structure of **2**. M−L bond lengths were modeled after those found for the TBP *cis*-dioxo complex $(Ph_3P)_2N[O_2RuCl_3]$,[13] the SP model reflecting only the shorter of the two lengths.

(22) Rossi, A. R.; Hoffmann, R. *Inorg. Chem.* **1975**, *14*, 365−374.

(23) ^{1}H-NMR was performed on a Varian 300 MHz FT-NMR with benzene-d_6 as solvent. Benzene backbone H, 6.7 and 8.3 ppm (q); gem diphenyl H, 7.6 and 7.7 ppm (d), 7.0−7.1 ppm (m).

(24) Holm, R. H.; Donahue, J. P. *Polyhedron* **1993**, *12*, 571−589.

(25) Kirklin, D. R.; Domalski, E. S. *J. Chem. Thermodyn.* **1988**, *20*, 743−745.

(26) Two CH_2Cl_2 solutions (25 mL) containing equal concentrations of Ph_3P, one containing 10−20 mg of **1**, were stirred at room temperature under a constant flow of air in flasks fit with water-cooled condensers. ^{31}P-NMR (Ph_4PCl as standard) showed an average turnover of 306 Ph_3P═O/Ru.